



## Adhesive joint formation between porous wood adherends with one-component polyurethane part 2

Adrian Wick, Martin Lehmann & Thomas Volkmer

To cite this article: Adrian Wick, Martin Lehmann & Thomas Volkmer (17 Sep 2025): Adhesive joint formation between porous wood adherends with one-component polyurethane part 2, The Journal of Adhesion, DOI: [10.1080/00218464.2025.2550786](https://doi.org/10.1080/00218464.2025.2550786)

To link to this article: <https://doi.org/10.1080/00218464.2025.2550786>



© 2025 The Author(s). Published with license by Taylor & Francis Group, LLC.



Published online: 17 Sep 2025.



Submit your article to this journal [↗](#)



Article views: 179




View related articles [↗](#)



View Crossmark data [↗](#)

# Adhesive joint formation between porous wood adherends with one-component polyurethane part 2

Adrian Wick , Martin Lehmann, and Thomas Volkmer

Institute for Building Materials and Bio-based Products, Bern University of Applied Sciences- Architecture, Wood and Civil Engineering, Biel, Switzerland

## ABSTRACT

Performance of an adhesive bond depends on the individual strengths of the adherends, the adhesion of the interface layers, and the cohesion of the adhesive itself. Treating wood with liquids prior to bonding can displace air and impurities from the cell surface, and ensure that moisture-sensitive adhesives adhere properly. To understand the influence of the wetting agent, temperature and airing time on one-component polyurethane bonding, the bond quality was quantitatively assessed using tensile shear tests EN 302–1. Supplemented by light microscopy images of the bond design, it was possible to make statements about the bond geometry in relation to strength. It became clear that wetting has a significant influence on the penetration behaviour of the adhesive and thus has a key effect on the thickness of the glue line. As a result, the bond line thickness increases on average by 19 % when the airing time is extended by two minutes. Deeper penetration and reduction in voids are associated with the forcing of a vapour diffusion flow towards the centre of the board, which is intensified by the increase in the moisture conductivity coefficient with rising temperature. Therefore, the amount of adhesive required depends not only on the wood density, but also on wetting parameters.

## ARTICLE HISTORY

Received 18 March 2025  
Accepted 13 August 2025

## KEYWORDS

Wood bonding; 1C-PUR; wetting agent; wetting temperature; airing time, adhesive joint formation

## 1. Introduction

The bonding of wood is influenced by many factors, as already explained in various publications, e.g.<sup>[1–4]</sup> Of particular significance is the parameter surface treatment with liquids, e.g., water or primers, especially when bonding with the moisture-sensitive adhesive 1C-PUR. This is notably evident in the durability of the bonds assessed through delamination testing.<sup>[5,6]</sup> Moreover, for wood types that are difficult to bond, mainly hardwoods and resin-rich softwoods, pre-treatment with liquid is often prescribed in the approval.<sup>[7]</sup> The general behaviour of liquids in wood is therefore explained in more detail,

**CONTACT** Adrian Wick  [adrian.wick@bfh.ch](mailto:adrian.wick@bfh.ch)  Institute for Building Materials and Bio-based Products, Bern University of Applied Sciences- Architecture, Wood and Civil Engineering, Solothurnstrasse 102, Biel CH-2504, Switzerland

© 2025 The Author(s). Published with license by Taylor & Francis Group, LLC.

This is an Open Access article distributed under the terms of the Creative Commons Attribution License (<http://creativecommons.org/licenses/by/4.0/>), which permits unrestricted use, distribution, and reproduction in any medium, provided the original work is properly cited. The terms on which this article has been published allow the posting of the Accepted Manuscript in a repository by the author(s) or with their consent.

followed by a listing of effects on wood surfaces caused by liquids, and finally a consideration of the bonding mechanism of 1C-PUR.

In wood, which is a porous, hygroscopic adherend, the use of liquids for surface treatment can trigger various processes. In the capillary-porous wood system, moisture movement is caused by vapour pressure gradients. Water evaporates from the menisci under load, diffuses into air-filled pores, and condenses on opposite menisci that are not under load. The condensed water is transported in the menisci by tension differences. As long as there is a moisture difference in the wood, water is drawn out of the larger capillaries (tracheids, vessels) by the tensile forces and stored in the finest capillaries in the cell wall system. The moisture transport described takes place for a moisture range of 5 % up to fibre saturation point (FSP).<sup>[8,9]</sup> Above the FSP, the moisture is stored in the macrosystem and transported longitudinally to the fibre via the cavities of the vessels or fibres and transversely to the fibre through the pits (tangential) and rays (radial). The change in the transport process is based on a serial distinction between micro- and macro-systems at the FSP according to Tiemann.<sup>[10]</sup> However, current research indicates a parallel change.<sup>[11]</sup> This means that free water precipitates before the cell wall is fully saturated. The conduction of the fluid depends on the anatomical direction, the intensity and speed primarily on the distribution of the capillaries, the temperature, the viscosity, and the surface tension.<sup>[8,9]</sup> Water conduction can be expressed using the moisture conductivity coefficient  $K_{F,T}$  (1), which tends towards zero in wood at low moisture content and towards infinity in the area of water saturation. In the fibre saturation range, there is a local maximum, which describes the transition from the micro to the macro system. The moisture conductivity coefficient is proportional to the surface tension and inversely proportional to the viscosity of the liquid, which is why the influence of the temperature can be taken into account via the correction factor  $CF_T$ , whereby the moisture conductivity coefficient can be expressed as follows<sup>[12,13]</sup>:

$$K_{F,T} = K_{F,0} \cdot \frac{\eta_0}{\eta_T} \cdot \frac{\sigma_T}{\sigma_0} = K_{F,0} \cdot CF_T \quad (1)$$

$\eta_0, \sigma_0$  :Viscosity or surface tension at 0 °C

$\eta_T, \sigma_T$  :Viscosity or surface tension at T °C

$K_{F,0}, K_{F,T}$  :Moisture conductivity coefficient at 0 °C or T °C [kg/(m·s·%)]

$CF_T$  :Correction factor in depending on the liquid and temperature [-]

The viscosity  $\eta_T$ <sup>[14]</sup> and surface tension  $\sigma_T$ , according to the Eötvös approximation<sup>[15]</sup>, of water can be computed in dependence of the temperature by the following equations:

$$\eta_T = \frac{1}{0.1 \cdot T^2 - 34.335 \cdot T + 2472} [\text{Pa} \cdot \text{s}] \quad (2)$$

$$\sigma_T = 0.07275 \cdot (1 - 0.002 \cdot (T - 291)) [\text{N/m}] \quad (3)$$

Inserting the values derived from Equations (2) and (3) into Equation (1) yields a correction factor  $CF_T$  of approximately 1–5 for a temperature range of 0–100 °C. The correction factor shows a quadratic (approximately linear) increase with temperature, which consequently leads to an enhanced moisture conductivity coefficient by increasing the temperature. This approach can therefore also be applied to other liquids or the adhesive itself. In the field of adhesives, it is already known that its increased adhesive temperature during wetting and curing generally leads to a higher and more durable adhesive strength. In most cases, higher adhesive temperatures reduce viscosity and therefore facilitate wetting.<sup>[16]</sup>

Wood surfaces are treated with liquids before further processing for a variety of reasons. The wetting of wood surfaces is mainly known in the area of surface coating with paints or varnishes.<sup>[17]</sup> This involves wetting the surface with water in order to loosen the compacted wood surface via a relaxation and set-recovery process, which can lead to the fibres standing up.<sup>[18]</sup> The set recovery process is clearly visible in densified wood.<sup>[19]</sup> Local compression also occurs during the production of the wood surface, depending on the process, e.g., planing, sanding, feed rate, or cutting geometry.<sup>[9,20]</sup> Böger et al.<sup>[21]</sup> studied the interactions between wood and water in primers and found that initial moistening and reconditioning increased the original thickness of the lamella. This is attributed to the relaxation of previously compressed wood cells caused by mechanical surface processing. Treatment with water or primer leads to a measurable reduction in the modulus of elasticity of the wood. This can cause a local plasticisation, which changes the stress distribution in the bond line and thus potentially improves the overall bond performance.<sup>[22]</sup> An additional effect of watering is the opening of the pores.<sup>[9]</sup> The low-viscosity property of the water allows it to flow and penetrate into the cracks and cells of the wood surface. This can be used to displace air and impurities on the cell surface.<sup>[20]</sup> When bonding wood with moisture-sensitive adhesives, such as one-component polyurethane (1C-PUR), the moisture content of the wood plays a decisive role in the curing process.<sup>[23]</sup> This is because 1 mole of a reactive isocyanate group requires 18 g of water for curing.<sup>[24]</sup> In the case of polyurethane adhesives, the absence of moisture increases the curing time.<sup>[25]</sup> In non-air-conditioned rooms, the relative humidity can fall below 30 % during the winter months, causing the wood surface to dry out considerably within a few hours.<sup>[26]</sup> In addition, low wood moisture can lead to a permanent loss of the available polar hydroxyl groups, which reduces wetting by polar liquids. Removing the bound water

from the cell wall brings the cellulose chains close enough together to form intramolecular bonds. This effect is also responsible for the hysteresis behaviour of the wood equilibrium moisture content.<sup>[27]</sup> The moisture absorption in the wood leads to swelling, which exposes further adsorption sites. The additional adsorption sites increase the surface energy of the wood and thus the critical surface tension<sup>[20],[28]</sup>. As the penetration depth of 1C-PUR is quite shallow, the adhesive lacks the necessary water for curing<sup>[26]</sup>. Preliminary water spraying at substrate or surface moisture levels below 8 % significantly improves the performance of the adhesive.<sup>[1,29]</sup> This effect increases up to 50 g/m<sup>2</sup> of applied water for systems with low reactivity (waiting time 60 min), reaches a maximum at 34 g/m<sup>2</sup> for medium reactivity (waiting time 30 min) and has a slightly negative effect for highly reactive adhesive systems (waiting time 0 min)<sup>[26]</sup>. Investigations into the wood-water interaction of primers in 1C-PUR bonding have shown that primers improve the bulk flow, leading to a better penetration of the adhesive into the voids and thus to a reduction in the glue line thickness, which results in better tensile strength.<sup>[21]</sup> Atomic force microscopy revealed that water-based primer systems exhibited significantly enhanced adhesion compared to unprimed surfaces.<sup>[30]</sup> The study by Luedtke et al.<sup>[31]</sup> reveals a glue line thickness of  $20 \pm 9 \mu\text{m}$  for circumferentially surface milled beech wood with a density of  $740 \pm 50 \text{ kg/m}^3$ , primed with 20 g/m<sup>2</sup> of Loctite PR 3105 and aired for 10 minutes, bonded with 160 g/m<sup>2</sup> of Loctite HB S109 adhesive at a pressure of 0.8 MPa. Tests on 1C-PUR glued finger joints, produced at a wood moisture content of 100 % and 14 %, show higher adhesive penetration and less blistering in the glue line.<sup>[32]</sup>

The Bonding corresponds to a composite material whose overall strength depends on the individual strengths of the adherends, the interface layers and the adhesive.<sup>[33]</sup> Adherends with higher strengths have higher bond strengths under the same conditions. This is due to the lower adhesive layer deformation resulting from the lower elongation at a higher modulus of elasticity. The strength of the interface and adhesive layers depends on the adhesion and cohesion forces acting on them.<sup>[24]</sup> Cohesive forces are present in all liquid and solid materials. Their magnitude determines the dimensional stability of a material. Ideally, an adhesive bond should have uniform cohesive strength across the entire glue line. Incorrect ratios of the components, air bubbles caused by the mixing or curing processes, significant variations in the thickness of the glue line or disregard the specified curing time or temperature have an adverse effect.<sup>[34]</sup> Wood undergoes constant shrinkage and swelling due to its hygroscopic material behaviour, which leads to additional internal stresses, especially at material transitions. However, this behaviour can be mitigated by the use of either stiff in-situ polymerised adhesives (MUF, PRF), which stabilise the material transition by infiltrating the cell walls, or elastic pre-polymerised adhesives (1C-PUR), which adapt better to deformations due to their flexibility.<sup>[35]</sup> Improved force transmission through the adhesive layer

can be achieved by reducing any stress peaks. The more an adhesive layer can compensate for these stress peaks through elastic and/or plastic deformation, the greater the proportion of the adhesive surface that transfers the load. This allows the potential of the cohesive strength to be exploited to a greater extent.<sup>[24]</sup> The working range of adhesion forces is defined as an interface layer. The various wood adhesives can mainly be divided into three categories according to their adhesion mechanisms: mechanical, chemical or physical. Mechanical adhesion involves anchoring the cured adhesive in the cell- and intercellular cavities, micropores of the cell walls or on the surface, which is enabled by roughness. In addition to the roughness of the wood and the viscosity of the adhesive, absorption plays an important role in mechanical interlocking. It influences the penetration of liquids into pores and irregularities on adhere surfaces. Thus, higher absorptions produce better adhesion in mechanical interlocking systems.<sup>[36,37]</sup> Secondly, an adhesion mechanism is physical when it is based on Van der Waals forces, hydrogen bonds or electrostatic interactions. Wood as an adherend provides free hydroxyl groups, which are a prerequisite for the formation of hydrogen bonds. The third category is the chemical adhesion, which is described by a covalent bond between the molecules of the wood and the adhesive.<sup>[16,24,38,39]</sup> Since the wood components (cellulose, hemicellulose and lignin) contain varying amounts of hydroxyl groups, it is theoretically possible to develop a urethane bond with the wood when bonding with 1C-PUR. Studies have shown that in the presence of water, the reaction is dominated by the formation of a urea bond. The reason for this is the higher nucleophilicity of amines, which leads to a faster reaction of amine with isocyanate.<sup>[40]</sup> In an oven-dry state, a covalent urethane bond with the wood can be detected for phenyl isocyanate, whereby lignin reacts most quickly. However, 4,4-diphenylmethane diisocyanate (MDI), which is widely used commercially, shows the presence of an urethane bond (wood-isocyanate) up to a wood moisture content of 7%.<sup>[41]</sup> Urethane and urea intermediates contain one or two acidic hydrogen atoms that react with free isocyanate to form allophanates or biuret when energy is added. Due to the greater nucleophilicity of the urea group, biuret formation occurs uncatalysed at temperatures above 100 °C.<sup>[40]</sup> Thus, depending on the isocyanate prepolymer, the PUR adhesive bond to wood is composed of a small proportion of chemical adhesion and a larger proportion of physical and mechanical adhesion. For all adhesion components, good wetting of the joint surfaces is a prerequisite for successful bonding. The adhesion mechanisms described above can be activated more effectively when they are less influenced by a weak boundary layer (WBL). A WBL can occur in the form of mechanical WBL (e.g. trapped air bubbles, machining surface damage, or a dirty surface) and/or chemical WBL (e.g. lubricant contamination, plasticisers and/or additives, aged or inactivated surfaces and weathered surfaces).<sup>[42]</sup>

Since surface treatment with liquids has an influence on the condition of adherends, bulk flow and curing behaviour of adhesives, this research will investigate the influence of wetting agent and temperature as well as the set airing time in combination with a moisture-curing IC-PUR adhesive and beech wood. First, to identify the initial conditions, the influence of the amount of residual water in the wood is determined. Then, the effects on the cured adhesive bond are evaluated by using a tensile shear test. Finally, light microscopy images are used to establish correlations between strength and adhesive bond formation, along with drawing conclusions about changes in bulk flow. This is achieved by measuring the thickness of the glue line, the penetration depth, and check the homogeneity of the glue line in terms of bubbles.

## 2. Material and methods

In Europe, the use of face-bonded wood products (glued laminated timber, cross-laminated timber, etc.) for load-bearing purposes is linked to the successful classification of the adhesives used. The EN 302 test standards play an important role in this context. The results presented are based on the tensile shear strength according to EN 302-1<sup>[43]</sup> with treatment sequences A1 (no treatment except air conditioning at standard climate 20/65) and A4 (treatment 6 h boiling water and 2 h cooling water at 20 °C). The performance of one-component polyurethane adhesives for load-bearing timber components exposed to different climatic conditions is classified according to EN 15425.<sup>[44]</sup> For the application of adhesive class type I (service class 1–3), limit values for tensile shear tests of  $A1 = 10 \text{ N/mm}^2$  and  $A4 = 6 \text{ N/mm}^2$  are required. Different types of surface treatment variants were used to produce the various test specimens. In the first series, the temperature and type of liquid were varied while the airing time was kept constant. In the second series, the airing time was varied for the best commercially viable variant from series 1. The wood used, beech (*Fagus sylvatica*), was kiln-dried to a target moisture content of 11–12 % prior to conditioning the lamellas in the standard climate (20 °C and 65 % relative humidity) for at least 6 months. Except for the production of the surfaces and the pressing process, all work took place in a standard climate. The labels represent the test series of 20 samples each (10 × A1; 10 × A4), differing in the wetting agent used (tap water; demineralised (DM) water), temperature and airing time. The thickness planers used were both based on the principle of circumferential surface milling. The main parameters are summarised in the following [table 1](#):

## 2.1. Desorption behaviour of wetted wooden surfaces

The desorption tests on wetted surfaces are intended to demonstrate the influence of the wetting temperature on the transport process in wood, as described in the introduction. It also gives an indication of the additional amount of water available in the wood for curing the moisture sensitive adhesive 1C-PUR. As the curing rate of the adhesive depends on the temperature and therefore the adhesive viscosity changes, the surface temperature is also measured. Wetting the adherends with demineralised water (D20°, D55°, D85°) was carried out in isolated cases on beech boards. The beech board was previously stored in the climate [20/65] until mass constancy was reached. Consequently, a target quantity of 20 g/m<sup>2</sup> of demineralised water at a temperature of 20 °C, 55 °C and 85 °C was applied to a beech board using the E1850+ Standard spraying device from Spraying Systems Co. The wetting process could not take place in a normal climate, the corresponding room conditions were humidity of 43 % and a temperature of 17 °C. During the first 20 min, the weight change (Kern KB 2400-2N) and the temperature change (Scotchtrak Heat Tracer) were recorded at 1 min intervals.

**Table 1.** Summary of the main manufacturing parameters of the test specimens for tensile shear strength depending on the wetting agent (left) and the airing time (right) with the nominal values and actual values in brackets.

Label	T20°	T55°	T85°	D20°	D55°	D85°	D20°-2	D20°-4	D20°-6	D20°-8	
Standards							EN 302-1				
<b>Wood</b>							Beech				
-Cutting direction							Riftboard				
-Dimension l-w-t							2x(315x134x5)				
-Density [kg/m <sup>3</sup> ]				700 ± 50 (685 ± 24)			700 ± 50 (721 ± 36)				
-Wood moisture content [%]							12 ± 1				
<b>Manufacturing</b>							Thickness planer				
-Machine typ				Georg Fischer HD 65			Hoffmann D 512				
-Feed speed [m/min]				9			7				
-Infeed thickness [mm]				1			1				
-Tilt angle [°]				0			0				
-Cutting agent				Strip planing blade HSS			Tersa M+ HSS				
-Condition				new			new				
<b>Surface treatment<sup>1</sup></b>	Tap Water			Demineralised Water			Demineralised Water				
-Temperature [°C]	20	55	85	20	55	85	20				
-Concentration [%]							100				
-Amount [g/m <sup>2</sup> ]							20				
-Airing time [min]				10			2	4	6	8	
<b>Adhesive<sup>2</sup></b>							Loctite HB S109				
-Amount [g/m <sup>2</sup> ]							180				
-Application typ							Collano spatula				
Oxidation time <sup>3</sup> [min]				24 h (44.7 ± 23.7)			24 h (139.3 ± 55)				
Assembly time [min]				10			10				
-Open assembly time (OAT)				(2.0 ± 0)			(1.0 ± 0)				
-Closed assembly time (CAT)				(6.2 ± 1.27)			(4.1 ± 0.58)				
<b>Press</b>							Lindenberg Laborpresse KK				
-Pressing pressure [N/mm <sup>2</sup> ]							0.8				
-Pressing time [min]							25				

Note: <sup>1</sup>Tap water: According to, <sup>[45]</sup> Biel's lake water has a hardness of 10 °fH, pH value of 7.55 and a conductivity of 221 µS/cm. Internal measurements of the conductivity showed: tap water 362 ± 50 µS/cm, Demineralised water 9.2 ± 2.5 µS/cm.

<sup>2</sup>Technical data: Brookfield viscosity: 2-3x10<sup>5</sup> mPa·s at 20 °C; Density: 1.16 g/cm<sup>3</sup>; Solid content: 100 %.

<sup>3</sup>Corresponds to the time between the start of surface manufacturing and the start of adhesive application.

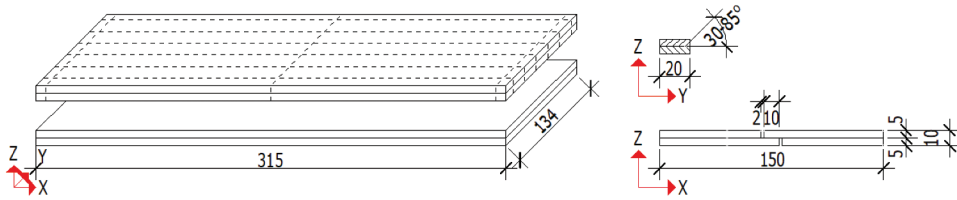


**Figure 1.** Bonded panel per variant ( $N_i=2$ ) and cutting of the test specimen ( $N_i=20$ ) according to EN 302-1.

## 2.2. Tensile shear strength

The bonding performance was analysed based on a tensile shear test in accordance with standard EN 302-1. Once the joining surface had been created using the processing parameters shown in Table 1, the 10 variants were wetted using the Autojet E185+ Spray System combined with a conveyer belt. Upon expiration of the airing time, two panels per variant were bonded with  $180 \text{ g/m}^2$  Loctite HB S109 Purbond adhesive according to the standard. The amount of adhesive corresponds to the maximum guide value according to the adhesive approval.<sup>[7]</sup> The adhesive was applied with a Collano spatula to the lower lamella. This area corresponds to the evaluation of the penetration depth of the adhesive on the lower side of the adhesive joint ( $t_{JP-L}$ ). The total assembly time (OAT+CAT) of 10 minutes and the pressing time of 25 minutes specified in the adhesive data sheet<sup>[46]</sup> were met for all variants, as shown in Table 1. Contrary to the pressure of  $1.2 \text{ N/mm}^2$  specified in the adhesive approval for surface bonding of beech wood,<sup>[7]</sup> the recommended pressure of  $0.8 \text{ N/mm}^2$  specified in the test standard is used for comparison purposes. After a post curing period of at least three days in a normal climate ( $20^\circ / 65\%$ ), the specimens were formatted to  $150 \times 20 \times 10 \text{ mm}$  before the  $10 \times 20 \text{ mm}$  test surface was created by precisely separating the first layer of wood and the adhesive layer with a 2 mm thick flat toothed saw blade (Figure 1). The resulting 20 test specimens were evenly distributed according to their density between treatment variants A1 ( $N_i = 10$ ) and A4 ( $N_i = 10$ ). As there is a significant difference in the stresses acting on the specimens, they were tested in dry A1 and wet A4 conditions. In the dry state, shear stresses predominate, whereas in the wet state, peeling stresses increase. In a water-saturated state (A4), the modulus of elasticity of wood is reduced by approx. 15 % compared to A1,<sup>[8]</sup> which leads to greater bending of the test specimens and increases the proportion of peel. The test specimens were tested with a clamping distance of 70 mm using a universal testing machine Z020 from Zwick Roell, force-controlled at 2 kN/min. The type of failure (cohesion, adhesion) was noted on the fracture surfaces and the percentage of fibre breakage was determined using the Wiesner test.

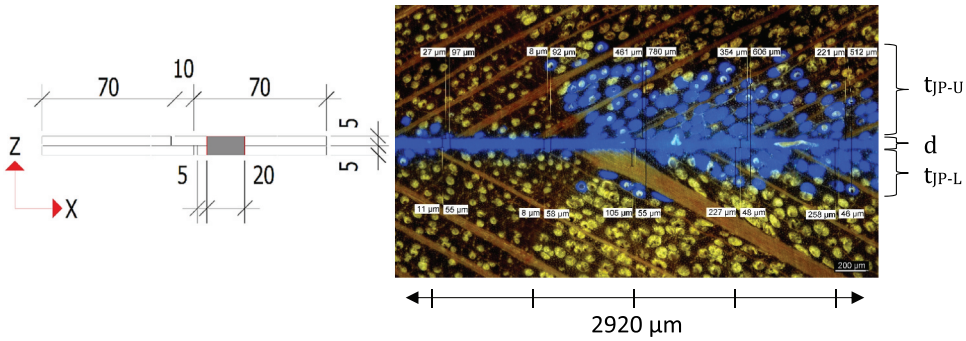


**Figure 2.** Left: position of the microscopy specimen; right: measurement of the adhesive joint using microscopy.

### 2.3. Adhesive joint design

Microscopic images were taken to analyse the distribution of the adhesive in the adhesive joint and to draw conclusions about the influence of surface treatment on bulk flow and bonding performance. Using a Leica DMLM light microscope with a magnification of five, as shown in Figure 2 on the right, a cross-sectional image was taken of each test specimen ( $N_i = 10 \cdot \bar{x}(x_1 \dots x_5)$ ) at a distance of 5 mm from the fracture surface (Figure 2 left) using the camera Jenoptik Gryphax Arktur. The adhesive contains a fluorescent component that can be clearly visualised with the aid of a UV light source. The Software Image Access was used to measure the upper ( $t_{JP-U}$ ) and lower penetration depth ( $t_{JP-L}$ ), the glue line thickness ( $d$ ), and the overall bond line thickness ( $t_{JP-U} + d + t_{JP-L}$ ) according to the definition of Marra<sup>[47]</sup> at five points (fixed pattern) in each case, taking into account the early and late wood (Figure 2 right). The measured values were calculated to an average value per test specimen ( $\bar{x}(x_1 \dots x_5)$ ).

### 2.4. Statistical analysis

Statistical analysis was performed using a two sample t-test with a 5 % significance level after checking the data for normal distribution using a Q-Q plot. The t-test was used to compare the means of the tensile shear strength as well as adhesive distribution. Descriptive statistics in the form of tables and box-whisker plots were used to further explain all the results. The box whisker plots used include the minimum (0th quantile) and maximum (4th quantile) as whiskers. The box from the 1st to the 3rd quantile describes the middle 50 % of the data divided by the median line (2nd quantile). Outliers are described as circles outside the whiskers, under condition that they are farther away than 1.5 times the interquartile range (3rd quantile minus 1st quantile). The mean is shown as an X.

### 3. Results

At the beginning, the desorption behaviour of the usual wetting quantity of  $20 \text{ g/m}^2$  is considered to classify the wetting process. The effects of wetting agent, wetting temperature and airing time are illustrated in the following sections 3.2 and 3.3 on the basis of specific results (strength, penetration depth, glue line thickness and adhesive joint design) in order to better understand their influence.

#### 3.1. Desorption behaviour of wetted wooden surfaces

The influence of the wetting temperature on the desorption behaviour and the surface temperature are analysed in Figure 3. The left one shows that the desorption behaviour of the wetting agents at a temperature of  $20^\circ\text{C}$  and  $55^\circ\text{C}$  is at a similar level for the first 7 minutes. After 10, 15 and 20 minutes the fitted difference increases from 2.5 % to 4.6 % and 7 % respectively. The desorption behaviour slows down as the temperature of the wetting agent increases. After just a few minutes, this leads to a difference in desorption behaviour when wetted with  $85^\circ\text{C}$  water compared to  $55^\circ\text{C}$  and  $20^\circ\text{C}$  wetting agent. The desorption of the fitted curve from  $85^\circ$  to  $55^\circ$  shows differences of 4.7 %, 8.8 %, 11.6 %, and 13.1 % after 5, 10, 15, and 20 minutes. When using a wetting agent at  $85^\circ\text{C}$ , about 48 % of the amount applied will remain on the board after 20 minutes of airing, compared to 28 % at  $20^\circ\text{C}$ . In general it can be seen that all three curves with a coefficient of determination  $R^2 > 0.99$  follow a 2<sup>nd</sup> degree polynomial quite exactly.

Looking at the surface temperature (Figure 3 right), it can be seen that the surface temperature for all three variants is  $22^\circ\text{C}$  before wetting. The wetting agent with a temperature of  $20^\circ\text{C}$  reduces the surface temperature to  $12^\circ\text{C}$  immediately after water application. After 13 min the surface starts to warm

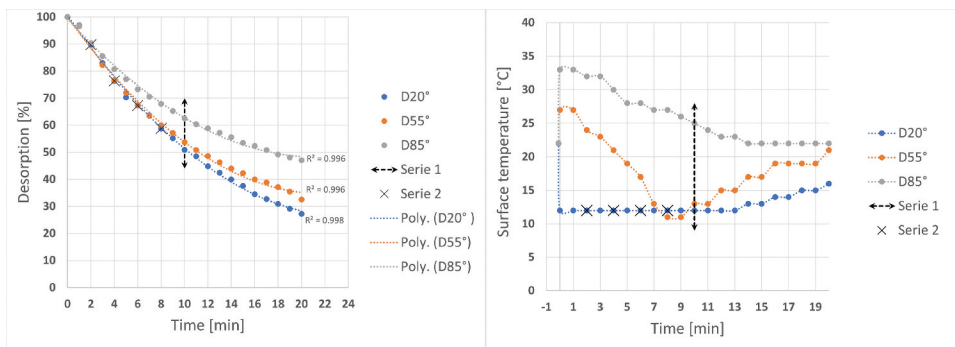


**Figure 3.** Left: desorption behaviour; right: surface temperature of beech boards wetted with an application quantity of  $20 \text{ g/m}^2$  ( $= 100 \%$ ) of demineralised water at a temperature of  $20^\circ\text{C}$ ,  $55^\circ\text{C}$  and  $85^\circ\text{C}$  for a time frame of 20 min.

up again and reaches 16 °C after 20 minutes. The wetting agent with a temperature of 55 °C initially increases the surface temperature to 27 °C and then drops to 11 °C within 7 minutes. After a holding time of 1 minute, the surface temperature rises to almost the initial temperature of the wood. The wetting agent with 85 °C water is the only wetting agent that does not show a drop below the initial temperature of the wood. It is depicted that the temperature can be increased to 33 °C with the wetting agent D85° and the initial temperature is reached again after just 14 minutes.

In summary, it can be said that for Series 1 with an airing time of 10 minutes, an additional amount of water is available with little variation in relation to the three wetting temperatures tested. After 10 minutes, at a wetting temperature of 85 °C, the surface temperature 25 °C is 5 °C higher than the temperature stated in the adhesive data sheet. This would indicate an accelerated reaction of the adhesive. On the other hand, the wetting temperatures of 20 °C and 55 °C show a reduction of 8 °C and 7 °C respectively, which would be associated with a reduction in the curing speed. For Series 2, with a variation in airing time of 2, 4, 6 and 8 minutes, there is a difference in the amount of water added of up to 30 %, while the surface temperature remains constant at 12 °C.

### 3.2. Wetting agent and temperature

This section presents the results for the evaluation of the influence of wetting agent ( $T$  = Tap water;  $D$  = Demineralised water) and wetting temperature (20 °C, 55 °C and 85 °C) on the adhesive performance and bond formation.

#### 3.2.1. Tensile shear strength

The results of the tensile shear strength tests after treatment A1 and A4 are shown in Figure 4 on the left. For all variants, the mean value with the corresponding standard deviation is  $14.2 \pm 1.9$  N/mm<sup>2</sup> for the dry-

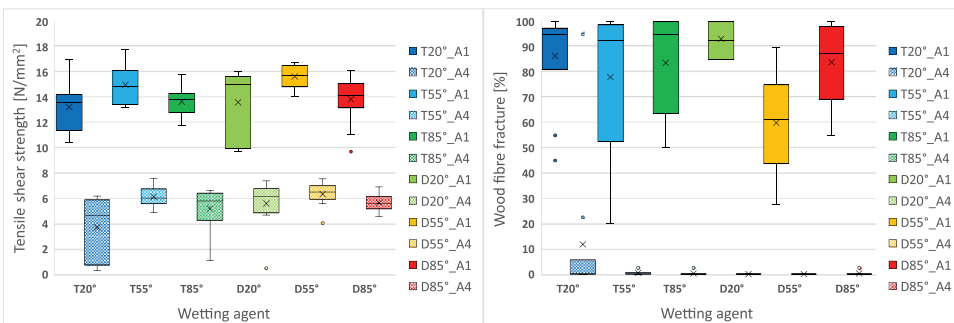


**Figure 4.** Left: tensile shear strength ( $N_i = 10$ ); right: fibre fracture percentage of the test specimens ( $N_i = 10$ ), divided into the tested wetting variants and treatment variants.

tested variants A1 and  $5.4 \pm 1.7$  N/mm<sup>2</sup> for the specimens after the boiling test A4. The mean values of all wetting variants of treatment A1 are above 10 N/mm<sup>2</sup> and therefore fulfil the above mentioned requirement. The variants with the wetting agent at 55 °C show a significant difference to the same wetting agent at temperatures of 20 °C and 85 °C. The required strength of 6 N/mm<sup>2</sup> after treatment A4 is only achieved for the two wetting agents at a temperature of 55 °C. Within the same wetting agent, there is only a significant difference between T20° and T55° for treatment A4.

The results from Figure 4, left, grouped in Table 2, show that there is no significant difference between the two wetting liquids for treatment A1, but a trend towards significance can be observed for A4 with  $p = 0.054$ . For treatment A1, the mean value with standard deviation is  $13.9 \pm 1.7$  N/mm<sup>2</sup> for tap water and  $14.4 \pm 2.2$  N/mm<sup>2</sup> for demineralised water. Treatment A4 shows a mean value with a standard deviation of  $5.0 \pm 2.0$  N/mm<sup>2</sup> for tap water and  $5.9 \pm 1.3$  N/mm<sup>2</sup> for demineralised water. In addition, an influence can be recognised when the temperature of the wetting agent is varied. For both wetting agents, the best result is obtained in all cases at a temperature of 55 °C.

The evaluation of the wood fibre fracture percentage (WFP) in Figure 4 right for A1 shows a mean value with a standard deviation of  $81 \pm 21$  %. Looking at the WFP per temperature level, it can be seen that at a wetting temperature of 20 °C the WFP ranges between 80–100 %. The wetting temperature of 55 °C shows the lowest WFP, whereby the variant D55°\_A1 standing out with an mean value of 60 %. In comparison with Figure 4 on the left, it can be seen that higher tensile shear strengths show lower WFP. At the 85 °C temperature level, the WFP is between 65 % and 100 %, which is between the 20 °C and 55 °C temperature levels. The variant D85°, with a median of 87.5 %, has the second lowest values after the D55° variant, viewed at the median level. This emphasises the comparatively good mean tensile shear strength of 13.9 N/mm<sup>2</sup> at a density of 668 kg/m<sup>3</sup>. The density of all other variants is on average 20 kg/m<sup>3</sup> higher. Generally, the fracture pattern is a combination of adhesive and cohesive fracture in the joint. Specimens with a high proportion of fibre fracture of 90–100 % show signs

**Table 2.** Tensile shear strength of the test specimens, divided into the tested wetting variants and treatment variants, given as mean value  $\pm$  standard deviation in the unit N/mm<sup>2</sup>.

Variant:	Wetter:	20 °C	55 °C	85 °C	Mean
A1	Tap water	$13.2 \pm 2.0$	$15.0 \pm 1.5$	$13.7 \pm 1.2$	$13.9 \pm 1.7$
	DM water	$13.6 \pm 2.7$	$15.7 \pm 0.9$	$13.9 \pm 2.0$	$14.4 \pm 2.2$
A4	Tap water	$3.7 \pm 2.4$	$6.1 \pm 0.8$	$5.2 \pm 1.7$	$5.0 \pm 2.0$
	DM water	$5.6 \pm 2.0$	$6.4 \pm 1.0$	$5.7 \pm 0.7$	$5.9 \pm 1.3$
Mean A1		13.4	15.35	13.8	$14.2 \pm 1.9$
Mean A4		4.65	6.25	5.45	$5.4 \pm 1.7$

of fibre deviation from the adhesive bond. With the exception of one test specimen, the fracture pattern of treatment A4 shows 0 % WFP throughout, which is reflected as an adhesion fracture. The outlier in the T20°\_A1 series experienced a failure in the wood plane due to the strong inclined fibres.

### 3.2.2. Adhesive penetration

The measured adhesive penetration depths into the lower (side of the adhesive application during production) and upper adherends are shown in Figure 5. In Figure 5 left, the bonds show a penetration depth in the upper adherend of around 60–300 µm, whereby the mean value with the standard deviation for treatment variants A1 and A4 is  $141 \pm 68 \mu\text{m}$  and  $140 \pm 83 \mu\text{m}$ . To analyse the penetration behaviour according to wetting agent and temperature, the values are grouped in Table 3. This shows that the upper penetration behaviour of both wetting agents is similar for the 20 °C and 85 °C temperature levels, whereby the mean penetration depth for the 85 °C temperature is around 35 µm greater. For the temperature level 55 °C, the penetration behaviour between the wetting agent tap water and demineralised water differs

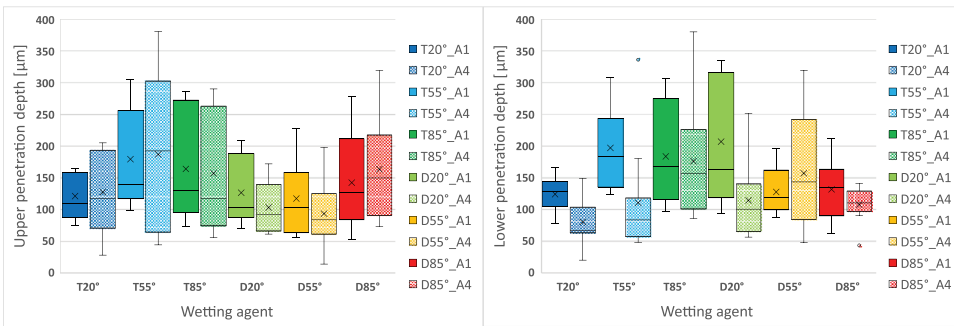


Figure 5. Left: upper; right: lower penetration depth of the adhesive, divided into the tested wetting variants and treatment variants ( $N_i = 10 \cdot \bar{x}(x_1 \dots x_5)$ ).

Table 3. Upper and lower penetration depth of the adhesive, divided into the tested wetting variants and treatment variants, given as mean value  $\pm$  standard deviation in the unit  $\mu\text{m}$ .

Variant		Wetter:	20 °C	55 °C	85 °C	Wetter	
Upper	A1	Tap water	121 $\pm$ 41	179 $\pm$ 63	164 $\pm$ 40	155 $\pm$ 73	
		DM water	126 $\pm$ 56	117 $\pm$ 55	142 $\pm$ 62	128 $\pm$ 60	
	A4	Tap water	127 $\pm$ 57	187 $\pm$ 95	157 $\pm$ 77	157 $\pm$ 95	
		DM water	113 $\pm$ 57	93 $\pm$ 48	163 $\pm$ 71	123 $\pm$ 68	
	<b>Mean</b>			<b>122 <math>\pm</math> 6</b>	<b>144 <math>\pm</math> 46</b>	<b>157 <math>\pm</math> 10</b>	<b>141 <math>\pm</math> 18</b>
	Lower	A1	Tap water	124 $\pm$ 31	197 $\pm$ 77	183 $\pm$ 54	168 $\pm$ 67
DM water			207 $\pm$ 58	127 $\pm$ 48	131 $\pm$ 38	155 $\pm$ 75	
A4		Tap water	79 $\pm$ 44	110 $\pm$ 65	176 $\pm$ 56	122 $\pm$ 86	
		DM water	114 $\pm$ 55	157 $\pm$ 70	107 $\pm$ 48	126 $\pm$ 69	
<b>Mean</b>			<b>131 <math>\pm</math> 54</b>	<b>148 <math>\pm</math> 38</b>	<b>149 <math>\pm</math> 37</b>	<b>143 <math>\pm</math> 22</b>	
Mean			127	146	153	142	
$\Delta$ (U-L)			-9	-4	+8	-2	

fundamentally. The tap water leads to the greatest penetration depth of all temperature levels and demineralised water to the smallest penetration depth of all temperature levels. The difference between the wetting agents is 62  $\mu\text{m}$  for treatment variant A1 and as much as 94  $\mu\text{m}$  for A4. On average, the demineralised water results in lower penetration depths for A1 and A4, but not to a statistically significant degree. The average value of both wetting agents increases by around 20  $\mu\text{m}$  per increase in temperature level (122  $\mu\text{m}$ ; 144  $\mu\text{m}$ ; 157  $\mu\text{m}$ ), with a significant difference only between temperature levels 20 °C and 85 °C.

For the penetration of the adhesive on the lower adherend (Figure 5 right), it can be seen that on average the penetration is at a comparable level for both wetting agents per treatment. However, the mean penetration value for treatment A4 is significantly lower with 124  $\mu\text{m}$  than for A1 with 161  $\mu\text{m}$ . No significant difference can be detected between the temperature levels of the lower penetration at the average level.

Both the upper and lower penetration depths show an influence of the temperature levels with a tendency for the penetration depth to increase with increasing wetting temperature. The test variant A1 and A4 has no effect on the upper penetration depth but has a significant effect on the lower penetration depth. The penetration depths for the top and bottom are at a similar level. This is confirmed by an almost identical overall mean value (all temperature levels, wetting agents and treatment variants) of  $141 \pm 18 \mu\text{m}$  at the top and  $143 \pm 22 \mu\text{m}$  at the bottom.

### 3.2.3. Glue line thickness

The grouped evaluation in Table 4 of the glue line thickness results as illustrated in Figure 6 indicates that the glue line is at a very similar niveau for all temperature levels and wetting agents. The thickness of the film ranges from 0–135  $\mu\text{m}$ , with an average value between 34  $\mu\text{m}$  and 84  $\mu\text{m}$ . Due to the wetting with the tap water, the adhesive has penetrated a partially deeper into the upper and lower parts. Consequently, there is now slightly less adhesive to form the glue line. Although the mean values of the individual temperature levels exhibit small variations, a discernible pattern emerges in the standard deviation of the four mean values. To illustrate this point, the mean value of the standard deviations ( $2 \times \text{A1} + 2 \times \text{A4}$ ) increases from 7.25  $\mu\text{m}$  to 7.75  $\mu\text{m}$

**Table 4.** Glue line thickness, divided into the tested wetting variants and treatment variants, given as mean value  $\pm$  standard deviation in the unit  $\mu\text{m}$ .

Variant:	Wetter:	20 °C	55 °C	85 °C	Mean
A1	Tap water	84 $\pm$ 7	34 $\pm$ 6	60 $\pm$ 14	59 $\pm$ 44
	DM water	49 $\pm$ 6	77 $\pm$ 8	78 $\pm$ 18	68 $\pm$ 58
A4	Tap water	70 $\pm$ 7	36 $\pm$ 8	59 $\pm$ 5	55 $\pm$ 42
	DM water	53 $\pm$ 9	83 $\pm$ 9	50 $\pm$ 11	60 $\pm$ 38
Mean		64 $\pm$ 16	58 $\pm$ 26	62 $\pm$ 12	61 $\pm$ 5

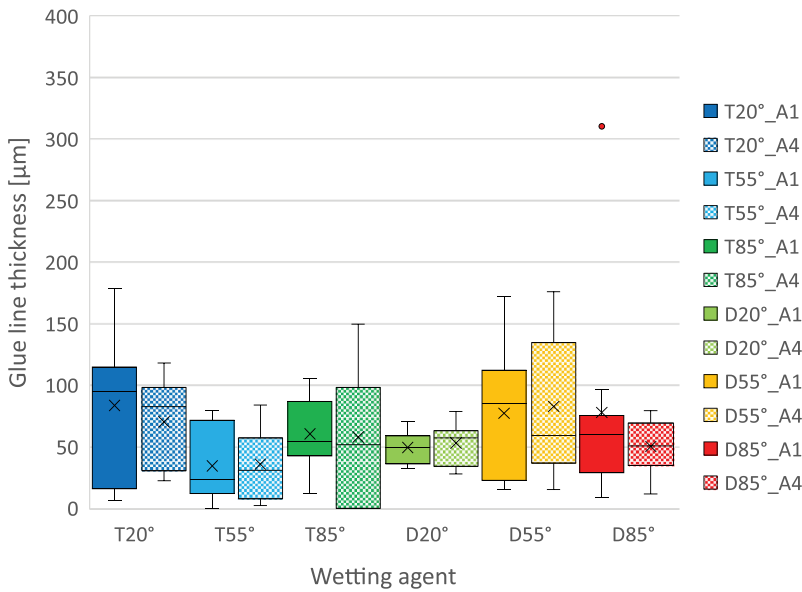


**Figure 6.** Thickness of the glue line between the joints, divided into the tested wetting variants and treatment variants ( $N_i = 10 \cdot \bar{x}(x_1 \dots x_5)$ ).

and even to 12  $\mu\text{m}$  as the temperature rises. It has been demonstrated that elevated wetting temperatures can have a negative impact on the flatness of the material. It can also be seen that the average thickness of the glue line across all wetting variants is  $61 \pm 5 \mu\text{m}$ , which corresponds to a thin glue line ( $\leq 0.1 \text{ mm}$ ) at a pressing pressure of  $0.8 \text{ N/mm}^2$  in accordance with standard EN 302-1.

### 3.2.4. Bond line thickness

The bond line thickness results in Figure 7 express the upper and lower penetration depths together with the thickness of the glue line. Most of the values are between 200–550  $\mu\text{m}$ . No pattern can be recognised from the specific mean value per temperature level, wetting agent and treatment variant (Table 5). Examining the mean values for each temperature level, averaged across wetting agents and treatments, reveals an increase in bond line thickness (39  $\mu\text{m}$ ) from 20 °C to 55 °C, followed by a slight increase (8  $\mu\text{m}$ ) from 55 °C to 85 °C. However, significant differences were only identified between temperatures 20 °C and 85 °C. The standard deviation is the inverse of to the mean value and decreases by around 10  $\mu\text{m}$  per temperature step. As can be seen from Figure 7 and Table 5, the adhesive with demineralised water as wetting agent has a smaller bond line thickness. Although this difference is statistically insignificant.

As a summary of the tested wetting variants, representative microscopic images with the corresponding joint design are shown in Table 6.

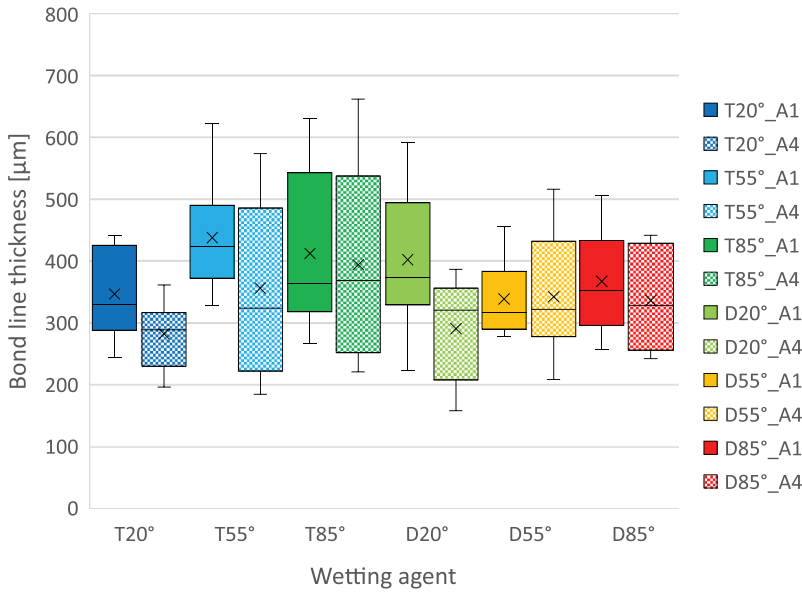


**Figure 7.** Thickness of the bond line, divided into the tested wetting variants and treatment variants ( $N_i = 10 \cdot \bar{x}(x_1 \dots x_5)$ ).

**Table 5.** Thickness of the bond line, divided into the tested wetting variants and treatment variants, given as mean value  $\pm$  standard deviation in the unit  $\mu\text{m}$ .

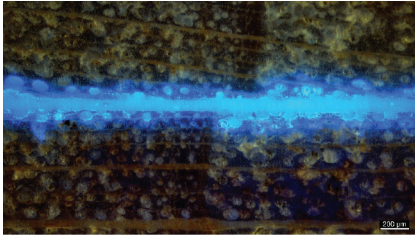
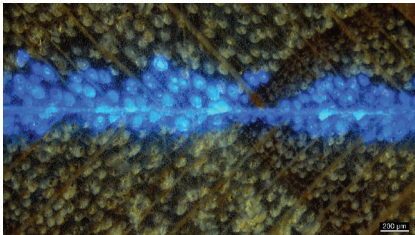
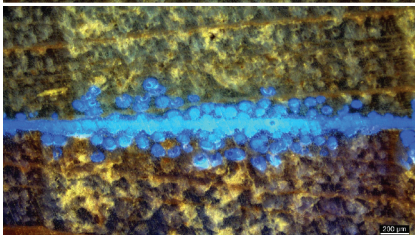
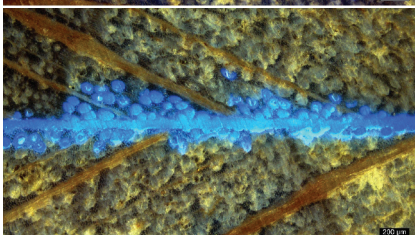
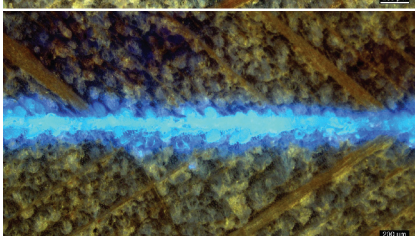
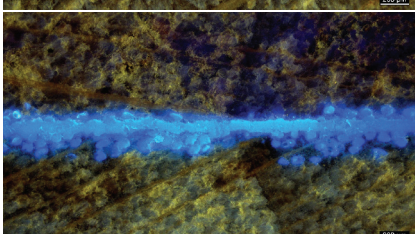
Variant:	Wetter:	20 °C	55 °C	85 °C	Mean
A1	Tap water	347 $\pm$ 42	438 $\pm$ 93	412 $\pm$ 68	399 $\pm$ 104
	DM water	402 $\pm$ 97	339 $\pm$ 82	367 $\pm$ 80	369 $\pm$ 109
A4	Tap water	282 $\pm$ 67	356 $\pm$ 126	394 $\pm$ 91	344 $\pm$ 148
	DM water	290 $\pm$ 86	342 $\pm$ 88	336 $\pm$ 85	323 $\pm$ 85
Mean		330 $\pm$ 56	369 $\pm$ 47	377 $\pm$ 33	359 $\pm$ 33

The joints at temperatures of 20 °C and 55 °C have a smooth surface. The joint specimens at the 85 °C temperature level show a slightly wavy surface. As all test specimens were produced with new planer knives, it can be assumed that the use of wetting agents at high temperatures can cause an uneven surface. The values described are average values ( $\bar{x} = \bar{x}_1(x_1 \dots x_5) \dots \bar{x}_{10}(x_1 \dots x_5)$ ) from treatment A1 and A4 in Figures 5–7.

### 3.3. Airing time of the wetting agent

In this results section, all bonding surfaces were wetted with demineralised water at a temperature level of 20 °C (D20°) prior to bonding. Subsequently, the airing time was varied between 2 min and 8 min with an interval of 2 min in order to study a possible influence on the bonding quality.

**Table 6.** Representative microscopic images of the average adhesive joint design parameter in relation to the wetting agent.

Variable:		Microscopic image:	Description:
Tap water	20 °C		Upper penetration depth: 198 μm Lower penetration depth: 149 μm Glue line thickness 24 μm Bond line thickness 380 μm Blister formation: none
	55 °C		Upper penetration depth: 183 μm Lower penetration depth: 153 μm Glue line thickness: 35 μm Bond line thickness: 397 μm Blister formation: none
	85 °C		Upper penetration depth: 160 μm Lower penetration depth: 180 μm Glue line thickness: 59 μm Bond line thickness: 403 μm Blister formation: none
Demineralsised water	20 °C		Upper penetration depth: 120 μm Lower penetration depth: 160 μm Glue line thickness: 51 μm Bond line thickness: 346 μm Blister formation: none
	55 °C		Upper penetration depth: 105 μm Lower penetration depth: 142 μm Glue line thickness: 80 μm Bond line thickness: 340 μm Blister formation: none
	85 °C		Upper penetration depth: 153 μm Lower penetration depth: 119 μm Glue line thickness: 64 μm Bond line thickness: 352 μm Blister formation: none

### 3.3.1. Tensile shear strength

The results of the tensile shear strength tests after treatment A1 and A4 are shown in [Figure 8](#) on the left and [Table 7](#). For all variants, the mean value with the corresponding standard deviation is  $14.4 \pm 1.8 \text{ N/mm}^2$  for the dry-tested variants A1 and  $6.3 \pm 1.5 \text{ N/mm}^2$  for the specimens after the boiling test A4. The mean values of all airing levels of treatment variant A1 are above  $10 \text{ N/mm}^2$  and therefore meet the requirements of EN 15425. The results show that the airing times has an influence on the tensile shear strength. This becomes apparent when comparing the airing times 2 min and 4 min, where the tensile shear strength in test method A1 remains constant with increasing density. The results of the 2-6 min airing time variant show significantly better values than at 8 min. The strengths after treatment A4 meet the requirement of  $6 \text{ N/mm}^2$  for the 2 min and 4 min airing variant. It is evident that the 4 min airing time variant has an exceptionally small standard deviation. The results of the 2-4 min airing show significantly better values than those of the 6-8 min airing.

By normalising the tensile shear strength to the density, the influence of the airing time can be better assessed. For treatment variant A1 it is evident that the results decline with increasing airing time, although the results remain stable between 4 min and 6 min. As with the non-normalised results, the difference between the results is only significant between 2–6 min compared to 8 min airing time. Similar to the non-normalised tensile shear strength,

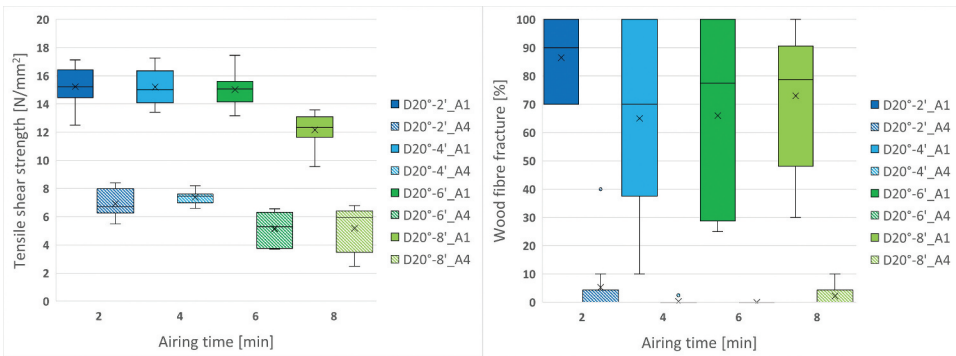


**Figure 8.** Left: tensile shear strength ( $N_i = 10$ ); right: fibre fracture percentage of the test specimens ( $N_i = 10$ ), divided into the tested airing times and treatment variants.

**Table 7.** Tensile shear strength of the test specimens, divided into the tested airing times and treatment variants, given as mean value  $\pm$  standard deviation in the unit  $\text{N/mm}^2$ .

Variant:	Airing time:				Mean
	2 min	4 min	6 min	8 min	
Density:	$716 \text{ kg/m}^3$	$755 \text{ kg/m}^3$	$744 \text{ kg/m}^3$	$673 \text{ kg/m}^3$	
A1	$15.2 \pm 1.4$	$15.2 \pm 1.3$	$15.0 \pm 1.2$	$12.2 \pm 1.1$	$14.4 \pm 1.8$
A4	$6.9 \pm 1.0$	$7.4 \pm 0.5$	$5.2 \pm 1.3$	$5.2 \pm 1.6$	$6.3 \pm 1.5$

there is a significant difference between the airing times of 2–4 min and 6–8 min for treatment variant A4. The results for the airing time of 2–4 min are at an identical level.

The evaluation of the wood fibre fracture percentage (WFP) in [Figure 8](#), on the right, shows for A1 an average value with a standard deviation of  $73 \pm 28$  %. It is noticeable that the test specimens with 2 min airing time exhibit a consistently high WFP of 70–100 %, without any external signs of inclined fibres. In general, the fracture pattern is characterised by a combination of adhesion and cohesion fracture in the bonded joint. The 4–8 min airing time variants show a cohesive failure in the adhesive for all test specimens with a wood WFP of less than 40 %. The results for treatment A4 show a very low WFP of  $2 \pm 7$  %, which is represented as adhesion fracture and largely as cohesion fracture in the adhesive.

### 3.3.2. Adhesive penetration

The measured adhesive penetration depths into the lower (side of the adhesive application during production) and upper adherends are shown in [Figure 9](#). In [Figure 9](#) left, the bonds show a penetration depth in the upper adherend of around 100–500  $\mu\text{m}$ , whereby the mean value with standard deviation for the A1 and A4 treatments being  $269 \pm 96$   $\mu\text{m}$  and  $260 \pm 165$   $\mu\text{m}$  respectively. The penetration depth for the D20°-6\_A4 variant differs from the rest and pushes the mean value for A4 upwards due to the high value. The statistical analysis shows no significant difference for treatment A1. In treatment A4, a difference can be seen between 2 min and 6 min or 8 min, as well as between 4 min and 6 min.

The penetration depth in the lower joint presented in [Figure 9](#) right ranges between 90–450  $\mu\text{m}$ , with a mean value with standard deviation of  $230 \pm 144$   $\mu\text{m}$  for A1 and  $201 \pm 151$   $\mu\text{m}$  for A4. The statistical analysis shows a significant difference between 2 min and 6 min and between 6 min and 8 min for treatment A1. In treatment A4, stages 2 min and 4 min, as well as 2 min and 6 min, are significantly different.

To analyse the penetration behaviour after airing time, the mean values of the upper and lower penetration depth are compared in [Table 8](#). There is a clear relationship between airing time and penetration depth. The penetration depth increases up to an airing time of 6 min, with a significant difference between 2 min and 4 min. The penetration depth for the 8 min airing time is less than for 6 min, but it is not entirely clear whether the peak was reached at 6 min or whether, in general, more adhesive is required to fill the lumina due to the lower density at 8 min airing time. The penetration depth at the bottom, where the adhesive is applied, is on average 40  $\mu\text{m}$  and 60  $\mu\text{m}$  less for A1 and A4 respectively, but with no statistical significance.

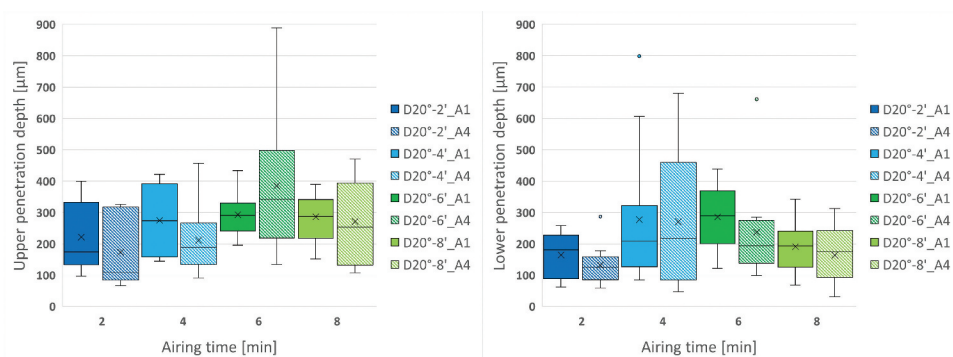


**Figure 9.** Left: upper; right: lower penetration depth of the adhesive, divided into the tested airing times and treatment variants ( $N_i = 10 \cdot \bar{x}(x_1 \dots x_5)$ ).

### 3.3.3. Glue line thickness

The glue line thickness illustrated in Figure 10 ranges mainly between 0–60  $\mu\text{m}$  with a mean value and standard deviation of  $14 \pm 19 \mu\text{m}$  for A1 and  $20 \pm 27 \mu\text{m}$  for A4. The grouped analysis in Table 9 shows that the glue line thickness decreases up to an airing time of 6 min, which supports the increasing penetration depth at the top and bottom. The increase in the glue line thickness for an airing time of 8 min suggests that the peak lies at an airing time of 6 min. In general, the glue line thickness is extremely low for all variants.

### 3.3.4. Bond line thickness

The bond line thickness results in Figure 11 on the left, expressing the upper and lower penetration depths together with the thickness of the glue line. The majority of the values are between 220–800  $\mu\text{m}$ . The bond line thickness increases up to and including the variant with 6 min airing time. There is a significant difference between 2 min to 4 min, 6 min and 8 min (except 2 min to 8 min treatment A1). Table 10 shows that an increase in density also increases the bond line thickness, as the existing cavity decreases. This can be seen by comparing the difference between the mean values in percent of

**Table 8.** Upper and lower penetration depth of the adhesive, divided into the tested airing times and treatment variants, given as mean value  $\pm$  standard deviation in the unit  $\mu\text{m}$ .

Variant:		Airing time:				Mean
		2 min	4 min	6 min	8 min	
Upper	A1	222 $\pm$ 94	275 $\pm$ 85	293 $\pm$ 151	286 $\pm$ 98	269 $\pm$ 96
	A4	174 $\pm$ 68	212 $\pm$ 65	386 $\pm$ 109	271 $\pm$ 113	260 $\pm$ 165
	<b>Mean</b>	<b>198</b>	<b>244</b>	<b>340</b>	<b>279</b>	<b>265</b>
Lower	A1	165 $\pm$ 79	277 $\pm$ 109	286 $\pm$ 141	191 $\pm$ 73	230 $\pm$ 144
	A4	132 $\pm$ 71	271 $\pm$ 96	237 $\pm$ 114	165 $\pm$ 54	201 $\pm$ 151
	<b>Mean</b>	<b>149</b>	<b>274</b>	<b>262</b>	<b>178</b>	<b>216</b>
Mean		174	259	301	229	241
$\Delta$ (U-L)		+49	–30	+78	+101	+49

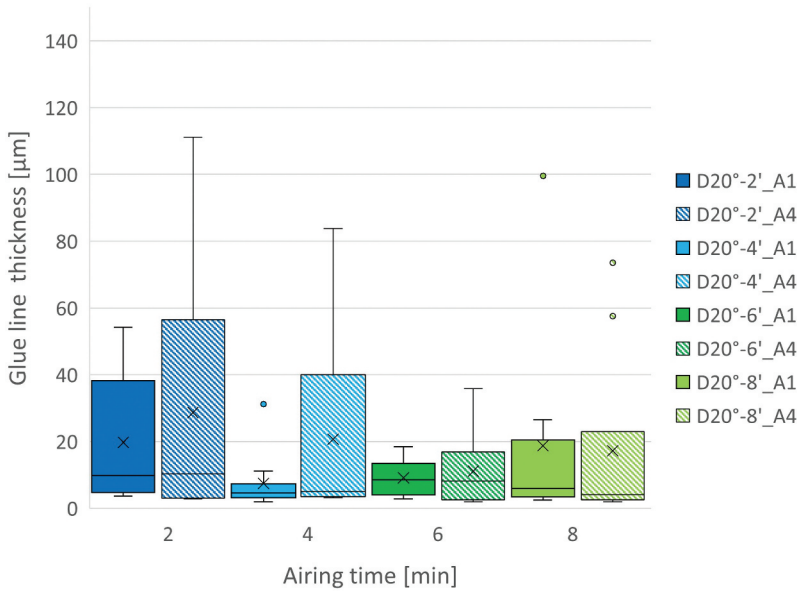


**Figure 10.** Thickness of the glue line between the joints, divided into the tested airing times and treatment values ( $N_i = 10 \cdot \bar{x}(x_1 \dots x_5)$ ).

**Table 9.** Thickness of the glue line between the joints, divided into the tested airing times and treatment variants, given as mean value  $\pm$  standard deviation in the unit  $\mu\text{m}$ .

Variant:	Airing time				Mean
	2 min	4 min	6 min	8 min	
A1	$20 \pm 4$	$8 \pm 2$	$9 \pm 2$	$19 \pm 4$	$14 \pm 19$
A4	$29 \pm 5$	$21 \pm 2$	$11 \pm 34$	$17 \pm 3$	$20 \pm 27$
Mean	25	15	10	18	17

bond line thickness and density. For this purpose, the change from 2–8 min for the bond line thickness and the density are plotted on the right hand side of Figure 11. It can be seen that there is a 100 % correlation between the change in density and the size of the bond line. In Table 10, the theoretical change in the bond line thickness is calculated using the linear equation from Figure 11 on the right. The difference between the measured change and the theoretically calculated change shows a change in the bond line thickness without the influence of density. This change shows a constant increase of  $19.2 \pm 0.14 \%$ .

Table 11 summarises the airing times tested and shows representative microscopic images with the corresponding joint design, respecting as far as possible the mean values on the right. It can be seen that with an airing time of 4 min or 6 min, the adhesive has penetrated to such an extent that only a very thin glue line remains. It can also be seen with these two variants that from a certain distance from the joint line, the lumina is only wetted with adhesive

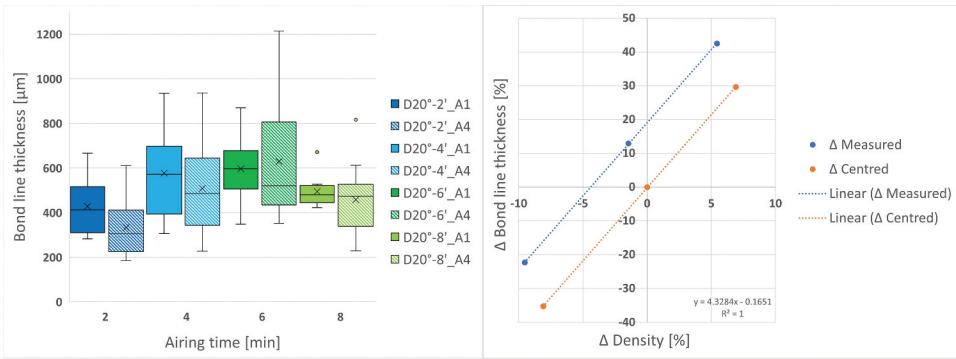


**Figure 11.** Left: thickness of the bond line, divided into the tested pressure levels and treatment variants ( $N_i = 10 \cdot \bar{x}(x_1 \dots x_5)$ ); right: comparison of the difference of the mean values in per cent of the adhesive area vs the density.

**Table 10.** Thickness of the bond line of the joint pieces, divided into the tested airing times and treatment variants, given as mean value  $\pm$  standard deviation in the unit  $\mu\text{m}$ .

Variant:	Airing time				Mean
	2 min	4 min	6 min	8 min	
A1	428 $\pm$ 139	577 $\pm$ 138	596 $\pm$ 190	494 $\pm$ 139	524 $\pm$ 1157
A4	333 $\pm$ 98	508 $\pm$ 134	629 $\pm$ 166	458 $\pm$ 128	482 $\pm$ 226
Mean	381	543	613	476	503
Density	716 $\text{kg}/\text{m}^3$	755 $\text{kg}/\text{m}^3$	744 $\text{kg}/\text{m}^3$	673 $\text{kg}/\text{m}^3$	721 $\pm$ 36 $\text{kg}/\text{m}^3$
Δ Density	+5.4 %	-1.5 %		-9.5 %	
Δ Bond line	+42.5 %	+12.9 %		-22.3 %	
Δ Theoretical	+23.4 %	-6.5 %		-41.5 %	
Δ w/o Density	+19.1 %	+19.4 %		+19.1 %	

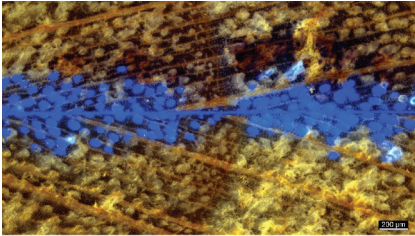
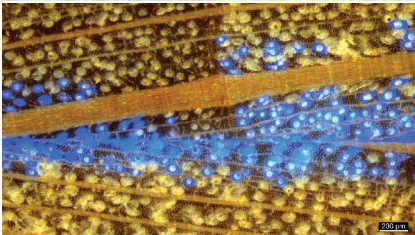
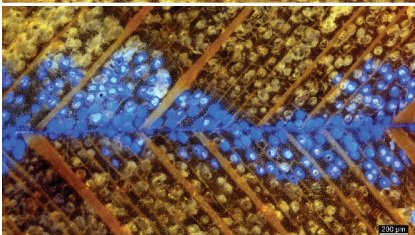
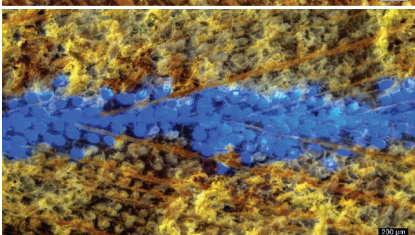
on the surface. The values described are average values ( $\bar{x} = \bar{x}_1(x_1 \dots x_5) \dots \bar{x}_{10}(x_1 \dots x_5)$ ) from treatment A1 and A4 in Figures 9–11.

#### 4. Discussion & conclusion

Before an adhesive system can be used to bond load-bearing timber products, the performance of the adhesive must be confirmed by standardised test methods. As adhesive bonds are mainly exposed to shear forces, the EN 302–1 standard, which involves analysing tensile shear forces, plays a central role in testing this property. To analyse the influence of different parameters on the quality of the bonded joint, it makes sense to use EN 302–1 as an evaluation standard. Microscopic images of the adhesive joint design can help to understand the mechanism of action of the tested parameters.

To evaluate the initial condition of the adherends after wetting at different temperatures, Chapter 3.1 showed the residual water content in the wood and the surface temperature using a desorption curve. For series 1, which had an airing time of 10 minutes, the differences in residual water content at the time

**Table 11.** Representative microscopic images of the average adhesive joint design parameter in relation to the airing time.

Variable:	Microscopic image:	Description:
Airing time of D20° -2 min		Upper penetration depth: 198 $\mu\text{m}$ Lower penetration depth: 149 $\mu\text{m}$ Glue line thickness: 24 $\mu\text{m}$ Bond line thickness: 380 $\mu\text{m}$ Blister formation: none
-4 min		Upper penetration depth: 243 $\mu\text{m}$ Lower penetration depth: 274 $\mu\text{m}$ Glue line thickness: 14 $\mu\text{m}$ Bond line thickness: 543 $\mu\text{m}$ Blister formation: none
-6 min		Upper penetration depth: 339 $\mu\text{m}$ Lower penetration depth: 262 $\mu\text{m}$ Glue line thickness: 10 $\mu\text{m}$ Bond line thickness: 613 $\mu\text{m}$ Blister formation: none
-8 min		Upper penetration depth: 279 $\mu\text{m}$ Lower penetration depth: 178 $\mu\text{m}$ Glue line thickness: 18 $\mu\text{m}$ Bond line thickness: 476 $\mu\text{m}$ Blister formation: none

of adhesive application were minor across the three temperature levels. These differences increased with longer airing times, indicating deeper penetration due to increased moisture conductivity at higher temperatures. Due to the reduced surface temperature of wetting agents D20° and D55° at the time of adhesive application, a reduction in reaction kinetics can be assumed. The opposite is true for the wetting agent at 85 °C. While the surface temperature of D55° rises rapidly again after a local minimum at 8–9 minutes, the surface temperature of D20° only recovers slowly after a constant plateau with a reduced temperature from 13 minutes onwards. This indicates that more energy is available to the system, particularly during the curing process with wetting agent D55°. While the amount of residual water at the time of adhesive application is comparable in series 1, the surface temperature remains constant for the different airing times (2 min; 4 min; 6 min; 8 min) in series 2.

Variation in airing time significantly influences the amount of residual water, mainly within the first 10 minutes (89 %; 78 %; 68 %; 59 %). Therefore, it can be concluded that the visible phenomena in series 2 are mainly due to mechanisms triggered by the amount of residual water.

In the processing of 1C-PUR, water is increasingly being used in industry to wet adherends, ensuring a proper curing of the moisture-curing adhesive system at low wood moisture levels. Therefore, the influence of wetting agents in the form of tap water and demineralised water at different temperature levels were investigated in Section 3.2. The results show that the penetration depth increases with the use of water as a wetting agent, which is consistent with the literature described in the introduction. One potential explanation for this behaviour is the wetting of the cell surface, which, on the one hand, enhances the accessibility of the adhesive, a phenomenon that has already been demonstrated in the literature with various other liquids. Alternatively, the behaviour may also be attributed to the transport of liquid into the wood structure. In the unwetted state, there is a moisture equilibrium and, by leaving the normal climate, the surface tends to dry out, which leads to moisture transport towards the surface. However, by wetting the surface, the transport direction is initially reversed. As described in the literature, there is a moisture difference in the wood as long as water is drawn out of the larger capillaries (tracheids, vessels) by the tensile forces and stored in the finest capillaries in the cell wall system. This can also be supported by the findings of microscopic images, where in addition to wetting in the vessels, filling of the small-pored structures is also observed. This indicates that mechanical adhesion is increased by stronger anchoring. The images also confirm the fact from the literature, as fewer blisters are formed with a higher moisture content. This aligns with previous literature suggesting that wetting with water reduces WBL consisting of trapped air. The influence of the reaction by-product, e.g., CO<sub>2</sub>, is ruled out, as an increased amount of water accelerates the reaction and promotes the accumulation of bubbles. However, it has also been shown that the penetration depth depends on the temperature of the wetting agent. While an increase in temperature from 20 °C to 55 °C significantly affects the penetration depth, a further increase to 85 °C does not yield additional effect. It is known from the literature that increasing the temperature enhances the moisture conductivity by reducing the viscosity and surface tension. This is confirmed by the desorption tests in section 3.1, which show that increasing the wetting temperature reduces the desorption rate. Hence, in series where the wetting agent and temperature were changed with an airing time of 10 minutes, more water is present at higher temperatures. This corresponds to a higher wood moisture content and therefore results in increased moisture conductivity. However, this does not explain the noticeably smaller difference in the penetration depth when increasing the temperature from 55 °C to 85 °C. However, the analysis of the measured surface temperatures indicates that at

a wetting temperature of 85 °C, the surface reaches a significantly higher thermal level and sustains it over an extended period. As the curing mechanism of 1C-PUR is increased at higher temperatures, it can be a possible explanation. Consequently, the wetting agent at 55 °C appears to provide an optimal temperature and moisture content, resulting in significantly better tensile shear strength after treatment A1 and A4.

The types of wetting agents have an impact on the penetration behaviour as outlined in section 3.2. It became obvious that the amount of the remaining wetting agent in the wood influences the bulk flow behaviour of the adhesive. Moreover, see section 3.3, the remaining wetting agent can intentionally be controlled by the airing time. The penetration depth increases steadily with an airing time of 2–6 minutes but reduces with an airing time of 8 minutes. This reduction in penetration depth is caused by the wood's lower density. This is confirmed by the linear correlation between the change in density and the change in bond line thickness. Hence, the penetration depth increases up to the maximum tested airing time of 8 minutes. An explanation for the corresponding behaviour has already been provided in the discussion for section 3.2 and is based on the build-up of a vapour pressure gradient with flow direction in the middle of the board. The behaviour of the tensile shear strength after treatment A1 shows that the drop in the variant with 4 minutes, resp., 6 minutes airing time is probably related to glue line thickness. While 25 µm remains in the variant with 2 minutes airing time, it is only 8–9 µm for 4–6 minutes. Compared to the values reported in the literature by Luedtke et al.<sup>[31]</sup> with adhesive joint thicknesses of  $20 \pm 9$  µm using 20 g/m<sup>2</sup> less adhesive under otherwise identical conditions, the influence is already considerable. With a glue line thickness of just a few micrometres (e.g., < 10 µm), local penetration of the wood into the glue line is to be expected. It causes a defect in the adhesive film, which leads to stress peaks and thus reduces the measured tensile shear strength. The same explanatory approach is valid for the values after treatment A4, where the worst values occur at a film thickness of 11 µm. The defect in the adhesive film resulted in an increased number of cohesion failures for variants with reduced adhesive thickness, as seen after an airing time of 4–8 minutes. This effect is more pronounced after treatment A4, due to the additional swelling pressure imposed on the moistened fibres in the glue line.

Combining tensile shear strength testing with microscopic image analysis was crucial for making well-founded statements about the impact of the adhesive joint quality on bond strength. Moreover, conclusions could be drawn about changes in the flow behaviour of the adhesive. Wetting the surface changes the penetration depth of the adhesive decisively depending on the wetting agent,

wetting temperature, and airing time. This also changes the thickness of the glue line. The change in density shows a linear correlation to the change in the bond line thickness. For the industry, this means that the influence on the adhesive should be known for the application of wetting agents, as in the worst case a reduction in bond strength is achieved. Based on this finding, future parameter studies on adhesive joints should be carried out with a very limited density of the test material. This is despite the fact that the EN 302–1 test standard for tensile shear test specimens allows densities of  $700 \pm 50 \text{ kg/m}^3$ . A follow-up study will investigate the influence of density and glue line thickness on strength.

## Acknowledgments

We would like to take this occasion to express our special thanks to Innosuisse, which made this scientific contribution possible by funding the research project. The data published here are part of Adrian Wick's master's thesis on the condition and treatment of the adhesive-wood interface.

## Author contributions

CRedit: **Adrian Wick**: Conceptualization, Investigation, Methodology, Writing – original draft; **Martin Lehmann**: Project administration; **Thomas Volkmer**: Funding acquisition, Supervision, Writing – review & editing.

## Disclosure statement

No potential conflict of interest was reported by the author(s).

## Funding

This document is the results of the research project funded by the Swiss Innovation Agency Innosuisse - Schweizerische Agentur für Innovationsförderung [49883.1 IP-EE].

## ORCID

Adrian Wick  <http://orcid.org/0009-0004-8949-6774>

## References

- [1] Wick, A.; Lehmann, M.; Volkmer, T. Adhesive Joint Formation Between Porous Wood Adherends with one-Component Polyurethane Part 1. *J. Adhes* 2025, 1–29. DOI: 10.1080/00218464.2025.2481107.
- [2] Hänsel, A.; Sandak, J.; Sandak, A.; Mai, J.; Niemz, P. Selected Previous Findings on the Factors Influencing the Gluing Quality of Solid Wood Products in Timber Construction and Possible Developments: A Review. *Wood Mater. Sci. Eng.* Mai 2021, 17(3), 230–241. DOI: 10.1080/17480272.2021.1925963.

- [3] Knorz, M. *Investigation of Structurally Bonded Ash (*Fraxinus excelsior* L.) as Influenced by Adhesive Typ and Moisture*; Doktor, Technische Universität München: München, 2015.
- [4] Hunt, C. G.; Frihart, C. R.; Dunky, M.; Rohumaa, A. Understanding Wood Bonds—Going Beyond What Meets the Eye: A Critical Review. *Int. J. Adhes. And Adhesives*, Bd 2018, 6(4), 369–440. DOI: 10.7569/RAA.2018.097312.
- [5] Böger, T.; Sanchez-Ferrer, A.; Richter, K. Hydroxymethylated Resorcinol (HMR) Primer to Improve the Performance of Wood-Adhesive Bonds – a Review. *Int. J. Adhes. Adhes. Bd März*, 2022, 113, S. 103070. DOI: 10.1016/j.ijadhadh.2021.103070.
- [6] Dill-Langer, G.; Nieberle, R.; Hänsel, A. Glued Laminated Robinia Hardwood Timber for Structural Use. *Bioresour. Bd Apr*, 2025, 20(2), S. 3848–3865. DOI: 10.15376/biores.20.2.3848-3865.
- [7] Bauaufsichtliche Zulassung: 1K-PUR-Klebstoffe LOCTITE HB S029 bis HB S1809 PURBOND für die Verklebung tragender Holzbauteile; Deutsches Institut für Bautechnik DIBt, Deutschland: Allgemeine bauaufsichtliche Zulassung/Allgemeine Bauartengenehmigung Z-9.1-765, 2024.
- [8] Niemz, P.; Sonderegger, W. *Holzphysik, 2. aktualisierte Auflage*; Fachbuchverlag Leipzig im Carl Hanser Verlag; München, 2017.
- [9] Wagenführ, A.; Scholz, F. *Taschenbuch der Holztechnik, 2. aktualisierte Auflage*; Fachbuchverlag Leipzig im Carl Hanser Verlag; München, 2012.
- [10] Tiemann, H. D. *Effect of Moisture Upon the Strength and Stiffness of Wood*; U.S. Dept. of Agriculture, Forest Service: Washington, DC, 1906. [Online]. Verfügbar unter: <https://archive.org/details/effectofmoisture70tiem/mode/2up>.
- [11] Fredriksson, M.; Thybring, E. E.; Zelinka, S. L.; Glass, S. V. The Fiber Saturation Point: Does it Mean What You Think it means? *Cellulose Feb*, 2025, 32(5), 2901–2918. DOI: 10.1007/s10570-025-06412-2.
- [12] Fortuin, G. *Anwendung mathematischer Modelle zur Beschreibung der technischen Konvektionstrocknung von Schnittholz*; Doktor, Univeristät Hamburg: Hamburg, 2003.
- [13] Kollmann, F. *Technologie des Holzes und der Holzwerkstoffe 1: Anatomie u. Pathologie, Chemie, Physik, Elastizität u. Festigkeit*, 2. Neubearb. u. erw. Aufl. 1951, Repr. In *Technologie des Holzes und der Holzwerkstoffe*; Springer: Berlin Heidelberg, 1982. 1050 p.
- [14] Höfler, A. Viskosität von Flüssigkeiten und Gasen. Zugegriffen: 30. Dezember 2022. [Online]. Verfügbar unter: <https://www.tec-science.com/de/mechanik/gase-und-fluessigkeiten/viskositat-von-fluessigkeiten-und-gasen/>.
- [15] Eötvös, R. Ueber den Zusammenhang der Oberflächenspannung der Flüssigkeiten mit ihrem Molecularvolumen. *Ann. Phys. Bd. Band 1886*, 263(3), S. 448–459. DOI: 10.1002/andp.18862630309.
- [16] Rasche, M. *Handbuch Klebtechnik*; Carl Hanser Verlag GmbH & Co. KG: München, 2012. DOI: 10.3139/9783446431980.
- [17] Kollmann, F. *Technologie des Holzes und der Holzwerkstoffe 2: Holzschutz, Oberflächenbehandlung, Trocknung und Dämpfen, Veredelung, Holzwerkstoffe, Spanabhebende und Spanlose Holzbearbeitung Holzverbindungen*, 2. Auflage. in Band 2; Springer Berlin Heidelberg: Berlin, Heidelberg, 1955. DOI: 10.1007/978-3-642-52947-4.
- [18] Gottlöber, C. *Zerspannung von Holz und Holzwerkstoffen*; Carl Hanser Verlag: München, 2014.
- [19] Scharf, A. *Advancing Continuous Surface Densification of Wood*; Doktorarbeit, Luleå University of Technology: Luleå, 2025.
- [20] River, B. H.; Vick, C. B.; Gillespie, R. H. *Wood as an adherend*, Bd. 7; Forest Products Laboratory: Madison, 1991.

- [21] Böger, T.; Engelhardt, M.; Suh, F. T.; Richter, K.; Sanchez-Ferrer, A. Wood-Water Interactions of Primers to Enhance Wood-Polyurethane Bonding Performance. *Wood Sci. Technol. Bd* 2023, 58(1), S. 135–160. DOI: [10.1007/s00226-023-01508-z](https://doi.org/10.1007/s00226-023-01508-z).
- [22] Böger, T.; Engelhardt, M.; Richter, K.; Sanchez-Ferrer, A. The Impact of Primers for Wood Bonding on Beech Wood's Young's modulus. *Eur. J. Wood Wood Prod. Bd* Feb, 2025, 83(1), 11. DOI: [10.1007/s00107-024-02165-0](https://doi.org/10.1007/s00107-024-02165-0).
- [23] Shirmohammadi, Y.; Pizzi, A.; Raftery, G. M.; Hashemi, A. One-Component Polyurethane Adhesives in Timber Engineering Applications: A Review. *Int. J. Adhes. Adhes. Bd* Apr, 2023, 123, S. 103358. DOI: [10.1016/j.ijadhadh.2023.103358](https://doi.org/10.1016/j.ijadhadh.2023.103358).
- [24] Habenicht, G. *Kleben: Grundlagen, Technologien, Anwendungen: mit 37 Tabellen, 5. erw. Aktualisierte Aufl. in VDI*; Springer: Berlin Heidelberg, 2006.
- [25] Hogger, E. M.; Bliem, P.; Griffith, R.; Van Herwijnen, H. W. G.; Stapf, G.; Konnerth, J. A Discussion on the Various Aspects of the Minimum Pressing Time for Polyurethane Adhesives. *J. Adhes. Bd* Feb, 2025, 101(3), S. 502–528. DOI: [10.1080/00218464.2024.2358076](https://doi.org/10.1080/00218464.2024.2358076).
- [26] Kägi, A.; Niemz, P.; Mandallaz, D. Einfluss der Holzfeuchte und ausgewählter technologischer Parameter auf die Verklebung mit 1K-PUR Klebstoffen unter extremen klimatischen Bedingungen. *Holz Als Roh- Werkst. Bd* Aug, 2006, 64(4), S. 261–268. DOI: [10.1007/s00107-005-0088-2](https://doi.org/10.1007/s00107-005-0088-2).
- [27] Niemz, P.; Teischinger, A., und Sandberg, D., Hrsg. *Springer Handbook of Wood Science and Technology. in Springer Handbooks*; Springer International Publishing: Cham, 2023. DOI: [10.1007/978-3-030-81315-4](https://doi.org/10.1007/978-3-030-81315-4).
- [28] Collett, B. M. A Review of Surface and Interfacial Adhesion in Wood Science and Related fields. *Wood Sci. Technol. Bd* 1972, 6(1), S. 1–42. DOI: [10.1007/BF00351806](https://doi.org/10.1007/BF00351806).
- [29] Beaud, F.; Niemz, P.; Pizzi, A. Structure–Property Relationships in One-Component Polyurethane Adhesives for Wood: Sensitivity to Low Moisture Content. *J. Appl. Polym. Sci. Bd* Sep, 2006, 101(6), S. 4181–4192. DOI: [10.1002/app.24334](https://doi.org/10.1002/app.24334).
- [30] Casdorff, K.; Kläusler, O.; Gabriel, J.; Amen, C.; Lehringer, C.; Burgert, I.; Keplinger, T. About the Influence of a Water-Based Priming System on the Interactions Between Wood and One-Component Polyurethane Adhesive Studied by Atomic Force Microscopy and Confocal Raman Spectroscopy Imaging. *Int. J. Adhes. Adhes. Bd* Jan, 2018, 80, S. 52–59. DOI: [10.1016/j.ijadhadh.2017.10.001](https://doi.org/10.1016/j.ijadhadh.2017.10.001).
- [31] Luedtke, J.; Amen, C.; van Ofen, A.; Lehringer, C. 1C-PUR-Bonded Hardwoods for Engineered Wood Products: Influence of Selected Processing Parameters. *Eur. J. Wood Wood Prod. Bd* März, 2015, 73(2), 167–178. DOI: [10.1007/s00107-014-0875-8](https://doi.org/10.1007/s00107-014-0875-8).
- [32] Aicher, S.; Reinhardt, H.-W., und Garrecht, H., Hrsg. *Materials and Joints in Timber Structures: Recent Developments of Technology, Bd. 9. in RILEM Bookseries*; Springer Netherlands: Dordrecht, 2014; Vol. 9. DOI: [10.1007/978-94-007-7811-5](https://doi.org/10.1007/978-94-007-7811-5).
- [33] Ehrhardt, M. *Untersuchung von Zugscherversuchen bezüglich der Eignung für GFK-Verklebungen im Schienenfahrzeugbau*; Masterthesis, Technische Universität Braunschweig: Braunschweig, 2020.
- [34] Habenicht, G. *Kleben - erfolgreich und fehlerfrei: Handwerk, Praktiker, Ausbildung, Industrie, Überarb. und erg. Aufl. in Studium Fertigungstechnik*; Vieweg + Teubner: Wiesbaden, 2012.
- [35] Frihart, C. R. Adhesive Groups and How They Relate to the Durability of Bonded Wood. *J. Adhes. Sci. Technol. Bd* Jan, 2009, 23(4), S. 601–617. DOI: [10.1163/156856108X379137](https://doi.org/10.1163/156856108X379137).
- [36] Cheng, E.; Sun, X. Effects of Wood-Surface Roughness, Adhesive Viscosity and Processing Pressure on Adhesion Strength of Protein Adhesive. *J. Adhes. Sci. Technol. Bd* Jan, 2006, 20(9), S. 997–1017. DOI: [10.1163/15685610677657779](https://doi.org/10.1163/15685610677657779).

- [37] Kim, W.-S.; Yun, I.-H.; Lee, J.-J.; Jung, H.-T. Evaluation of Mechanical Interlock Effect on Adhesion Strength of Polymer–Metal Interfaces Using Micro-Patterned Surface Topography. *Int. J. Adhes. Adhes. Sep.*, 2010, 30(6), 408–417. DOI: [10.1016/j.ijadhadh.2010.05.004](https://doi.org/10.1016/j.ijadhadh.2010.05.004).
- [38] Mittal, K. L., Hrsg *Progress in Adhesion and Adhesives*; John Wiley and Sons, Inc: Hoboken, New Jersey, 2015.
- [39] Brockmann, W.; Geiß, P. L.; Klingen, J., und Schröder, B., Hrsg *Klebetchnik, 1*; Weinheim: Aufl. Wiley-VCH, 2005. DOI: [10.1002/3527605851.fmatter](https://doi.org/10.1002/3527605851.fmatter).
- [40] Wirts, M. *Emission von Isocyanaten bei der Verarbeitung von Polyurethanklebstoffen*; Naturwissenschaftlichen Fakultät der Technischen Universität Carolo-Wilhelmina zu Braunschweig: Braunschweig, 2000.
- [41] Weaver, F. W.; Owen, N. L. Isocyanate-Wood Adhesive Bond. *Appl. Spectrosc.* Feb, 1995, 49(2), S. 171–176. DOI: [10.1366/0003702953963751](https://doi.org/10.1366/0003702953963751).
- [42] Pizzi, A. und Mittal, K. L., Hrsg *Handbook of Adhesive Technology*, 3rd ed.; CRC Press: Boca Raton, 2018.
- [43] *EN 302-1 Adhesives for Load-Bearing Timber Structures - Test Methods - Part 1: Determination of Longitudinal Tensile Shear Strength*; European Committee for Standardization: Brussels, 2023.
- [44] *EN 15425 Adhesives - One Component Polyurethane (PUR) for Load-Bearing Timber Structures - Classification and Performance Requirements*; European Committee for Standardization: Brussels, 2023.
- [45] Schweizerischer Verein des Gas- und Wasserfaches. Energie Service Biel. *trinkwasser.ch*; Zugriffen, Apr 15, 2025. [Online]. Verfügbar unter: <https://trinkwasser.ch/versorger/id:/supplier/:reading/:slug>.
- [46] Henkel & Cie AG, DS LOCTITE HB S109 PURBOND. Nov, 2021. <https://www.henkel-adhesives.com/at/de/industries/engineered-wood/engineered-wood-product-solutions.html>.
- [47] Marra, A. A. *Technology on Wood Bonding*; Principles in Practice, Van Nostrand Reinhold: New York, 1992.